



Since January 2020 Elsevier has created a COVID-19 resource centre with free information in English and Mandarin on the novel coronavirus COVID-19. The COVID-19 resource centre is hosted on Elsevier Connect, the company's public news and information website.

Elsevier hereby grants permission to make all its COVID-19-related research that is available on the COVID-19 resource centre - including this research content - immediately available in PubMed Central and other publicly funded repositories, such as the WHO COVID database with rights for unrestricted research re-use and analyses in any form or by any means with acknowledgement of the original source. These permissions are granted for free by Elsevier for as long as the COVID-19 resource centre remains active.



# Aerosols from speaking can linger in the air for up to nine hours

Shirun Ding, Zhen Wei Teo, Man Pun Wan, Bing Feng Ng<sup>\*</sup>

School of Mechanical and Aerospace Engineering, Nanyang Technological University, 50 Nanyang Avenue, 639798, Singapore

## ARTICLE INFO

### Keywords:

COVID-19  
Airborne transmission  
Speech aerosol  
Lifetime  
Respiratory diseases

## ABSTRACT

Airborne transmission of respiratory diseases has been under intense spotlight in the context of coronavirus disease 2019 (COVID-19) where continued resurgence is linked to the relaxation of social interaction measures. To understand the role of speech aerosols in the spread of COVID-19 globally, the lifetime and size distribution of the aerosols are studied through a combination of light scattering observation and aerosol sampling. It was found that aerosols from speaking suspended in stagnant air for up to 9 h with a half-life of 87.2 min. The half-life of the aerosols declined with the increase in air change per hour from 28 to 40 min ( $1 \text{ h}^{-1}$ ), 10–14 min ( $4 \text{ h}^{-1}$ ), to 4–6 min ( $9 \text{ h}^{-1}$ ). The speech aerosols in the size range of about 0.3–2  $\mu\text{m}$  (after dehydration) witnessed the longest lifetime compared to larger aerosols (2–10  $\mu\text{m}$ ). These results suggest that speech aerosols have the potential to transmit respiratory viruses across long duration (hours), and long-distance (over social distance) through the airborne route. These findings are important for researchers and engineers to simulate the airborne dispersion of viruses in indoor environments and to design new ventilation systems in the future.

## 1. Introduction

The transmission of some diseases (such as tuberculosis, measles, and chickenpox) via airborne routes has long been recognized [1]. For some respiratory viruses, such as SARS-CoV (Severe Acute Respiratory Syndrome CoronaVirus), MERS-CoV (Middle-East Respiratory Syndrome CoronaVirus) and influenza virus, their likelihood of airborne transmission is based on various indirect evidence or spreading events [2–4]. Correspondingly, for the continued resurgence of coronavirus disease 2019 (COVID-19), the prospects of airborne transmission have again come under intense spotlight [5,6]. This is supported by the detection of high viral loads of SARS-CoV-2 in oral fluids of asymptomatic and symptomatic COVID-19 patients [7,8]. Furthermore, the RNA of SARS-CoV-2 was detected in the aerosol samples of medical staff areas, isolation rooms, and toilets used by patients via polymerase chain reaction testing [9,10].

However, the relative significance of indirect airborne transmissions of virus-laden aerosols (also known as droplet nuclei) remains controversial in the context of COVID-19 [11–14]. Specifically, whether the aerosols are able to indirectly transmit viruses over social distances (e.g., 2 m) for prolonged periods of time via air movement as the third route of infection remains debatable [15,16]. This is in addition to the more widely recognized transmission via direct contact with patients and their respiratory droplets/aerosols within social distance [17], and

indirect contact with contaminated surfaces (i.e., fomites) or water or toilets (by fecal matter) [18–20]. Since aerosols are so small (e.g., <10  $\mu\text{m}$  after dehydration) that air current affects them more than gravitation [12,21,22], in contrast to droplets (e.g., >20  $\mu\text{m}$  after dehydration), the long-distance (>2 m) and long-time (hours) airborne transmission of aerosols might pose a higher risk in indoor environments [5,23,24]. In addition, virus-laden aerosols can enter deeper into the respiratory tract of the lungs, which may lead to higher severity of COVID-19 progression [10]. SARS-CoV-2 has been found to be transmittable via the air between two ferrets [16], but it is inconclusive whether the SARS-CoV-2 was transmitted through respiratory droplets, aerosols, or both. Gathering indisputable evidence for airborne transmission could take years and cost lives [11].

Considering that super-spreading events are more readily explained by long-range aerosol transmission [5], it is critical to understand the role of aerosols in the long-time and long-distance airborne transmission of viruses. In a recent study [15], the half-life of speech aerosols was reported to be from 8 to 14 min in a stagnant environment (23 °C, 27 % RH) via light scattering observation (LSO). However, the size information of the speech aerosols was not quantitatively obtained by the LSO measurements. In another recent study, “artificial” droplets with an average diameter of 5  $\mu\text{m}$  were sprayed into three rooms with different levels of ventilation, and the half-life of these droplets varied from 0.5 to 5 min via LSO [10]. However, human exhalation contains a wide range

<sup>\*</sup> Corresponding author.

E-mail address: [bingfeng@ntu.edu.sg](mailto:bingfeng@ntu.edu.sg) (B.F. Ng).

<https://doi.org/10.1016/j.buildenv.2021.108239>

Received 2 July 2021; Received in revised form 1 August 2021; Accepted 7 August 2021

Available online 8 August 2021

0360-1323/© 2021 Elsevier Ltd. All rights reserved.

of droplets (0.01–1000  $\mu\text{m}$ ), and aerosol particles are likely to linger in the air for a longer time [25,26].

To further understand the characteristics of speech aerosols that are responsible for airborne transmission of respiratory viruses, we measured the lifetime and size distribution of aerosols expelled from human speaking (corresponding to asymptomatic carriers) and coughing (corresponding to symptomatic carriers) in stagnant air and under three different levels of ventilation. As the aerosols and droplets from speaking or coughing contain a large particle size spectrum, a combination of LSO for medium-sized droplets ( $>2.45 \mu\text{m}$ ) and aerosol sampling measurements (10 nm–10  $\mu\text{m}$ ) was adopted with an elaborate chamber system (Fig. 1, Fig. A1 of Appendix). The use of LSO and aerosol measurement equipment (e.g., optical particle sizer) was discussed to be complementary in a previous study [15], but there is no experimental validation yet. Therefore, these two techniques will be used concurrently to explore their similarities and differences. In brief, a speaker speaks/coughs into a clean chamber ( $23 \pm 1^\circ\text{C}$ ,  $50 \pm 5\%$  RH) for  $\sim 10$  min, and the generated aerosol/droplets scatter a laser sheet, which is recorded by a camera. At the same time, the size-resolved

number concentration of aerosols in the chamber was sampled in real-time for the entire protocol.

## 2. Materials and methods

### 2.1. Air supply and chamber

A chamber with inner volume of  $0.5 \text{ m}^3$  was constructed out of stainless steel to minimize wall losses (Fig. 1). The interior of the chamber was covered with matte black vinyl film and the top was covered with a black cloth to reduce light pollution as much as possible for the experiments with LSO. Three inlets and three outlets were positioned on the sidewalls, and two fans were installed to promote the mixing of aerosols in the chamber. Two layers of sealing bags were attached to the speaking hole (13 cm diameter) of the chamber to prevent leakage of room air into the chamber during the experiments, especially for the speaking phase. Clean air was supplied to the chamber from the “air supply system” so as to create slightly higher pressure in the chamber to prevent dust from entering from the outside.

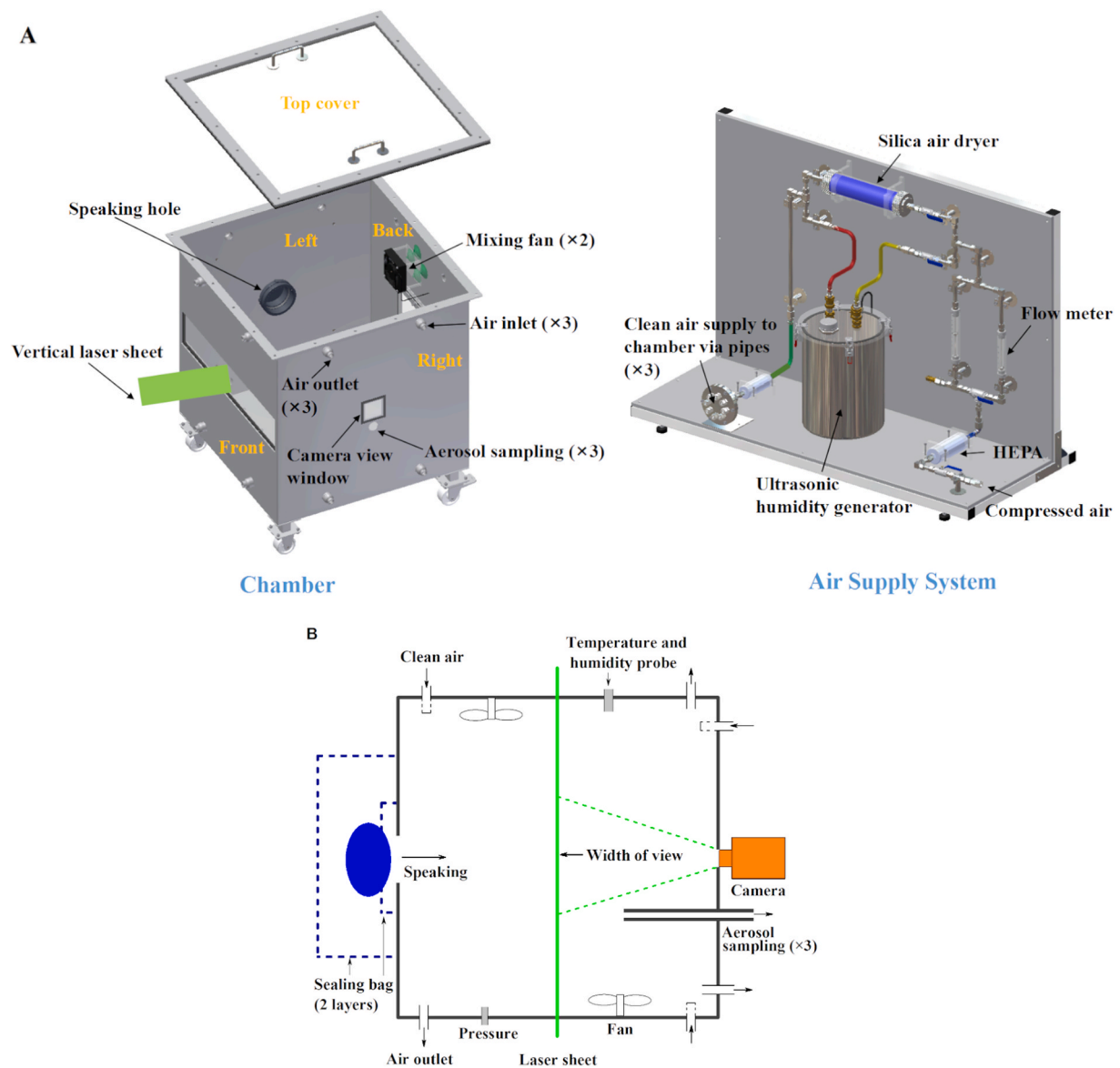


**Fig. 1.** Schematic of the experimental setup. (A) 3D schematics of a  $0.5 \text{ m}^3$  cubic stainless-steel chamber and air supply system. (B) The top view of the chamber system. A vertical laser sheet (height: 16.8 cm, thickness: 0.5 cm) is introduced through transparent windows across the chamber, normal to the speaking direction. A camera is located at the center of the right panel, with a hole for the speaker on the left panel.

In the “air supply system” in Fig. 1A, two high-efficiency particulate air filters with 99.97 % filtration efficiency at 0.3  $\mu\text{m}$  were used to remove particles from the compressed air. Prior to entry into the chamber, the humidity of supply air ( $50 \pm 5\%$  RH) was controlled by adjusting the mixing ratio of dried air and humid air from a humidity generator. The temperature of supply air ( $23 \pm 1^\circ\text{C}$ ) is typical of indoor environments. The measurements of temperature and relative humidity in the chamber were obtained using a sensor probe (TH210 BODI 150-R, KIMO) with a NI data logger (NI 9215) and LabVIEW NXG.

## 2.2. Light scattering observation

A 2 W, 532 nm continuous-wave diode-pumped solid-state laser was used in this experiment. The laser sheet produced was approximately 5 mm thick and 168 mm tall. Transparent windows on the front and rear panels allow for optical access to illuminate the measurement plane situated in the middle of the chamber (Fig. 1). A Canon EOS 800D camera with a Canon EF-S 18–135 mm f/3.5–5.6 lens was mounted 2 cm away from the 7 cm wide view window on the center of the right panel of the chamber. The camera was used to record 1080p videos ( $1920 \times 1080$  pixels resolution) at 25 frames per second. The focal length used was 35 mm, resulting in a field of view of  $\sim 30 \times 18$  cm, which was slightly larger than the illuminated area from the laser sheet. The camera was focused on the laser sheet, to continuously capture light that was scattered by aerosols. The effective volume of the laser sheet for aerosols captured in the videos is estimated to be  $252\text{ cm}^3$ . A MATLAB code was used to count the number of aerosols frame by frame whose maximum single-pixel intensity surpassed a threshold value of 15. Through several rounds of trial and error, it was observed that 15 provided adequate relevant information without having corruption from background noise. It should be noted that aerosols smaller than 15 are hence not captured.

## 2.3. Aerosol sampling equipment

A combination of particle sizers including a scanning mobility particle sizer (SMPS, size range: 10–420 nm, TSI 3910) and optical particle sizer (OPS, size range: 0.3–10  $\mu\text{m}$ , TSI 3330) was used to measure aerosol size distribution between 10 nm and 10  $\mu\text{m}$ . An ultrafine particle counter (P-Trak, size range: 20–1000 nm, TSI) was used as well. The sampling interval was 1 min for the SMPS, 1 s for both OPS and P-Trak. Three sampling pipes were inserted into the chamber by a depth of about 25 cm via an aerosol sampling hole on the right panel, as shown in Fig. 1.

## 2.4. Experimental procedure and conditions

The chamber was purged by clean air from the “air supply system” with mixing fans turned on for at least 1 h under air change per hour (ACH) of  $9\text{ h}^{-1}$ , until particle concentration ( $>10\text{ nm}$ ) in the chamber is near  $0\text{ \#}/\text{cm}^3$  before the start of experiments. Following which, measurements were recorded for the “background” phase from 0 to 14 min, which serves as a baseline. In the next  $\sim 10$  min, the speaker repeated the phrase “stay healthy” or coughed into the chamber via the inner layer of the sealing bag. Subsequently, the measurements continued to record for the “decay” phase of aerosols till they almost disappear. Note that the chamber was operated under ACH of  $9\text{ h}^{-1}$  in the “background” and “speaking” phases, and high positive pressure in the chamber prevented leakage of room air into the chamber from the speaking hole. Two mixing fans inside the chamber were turned on to promote the homogenous spatial distribution of aerosols in the “background” and “speaking” phases, which were turned off in the “decay” phase. The ACH of the chamber was set as 0 (i.e., stagnant air), 1, 4,  $9\text{ h}^{-1}$  in the “decay” phase (Table 1) by adjusting the flow rate of supply air to 0, 0.5, 2, and  $4.5\text{ m}^3/\text{h}$ , respectively, using the flow meter shown in Fig. 1A.

In Fig. 1B, two layers of sealing bags are attached to the speaking hole. The main function of the outer layer of the large sealing bag was to

**Table 1**

Summary of human exhalation types and experimental conditions.

exhalation type	loudness	environmental conditions in “background” and “speaking” phases	ACH ( $\text{h}^{-1}$ ) in “decay” phase <sup>d</sup>	air velocity near laser sheet (m/s) in “decay” phase <sup>e</sup>
speaking <sup>a</sup>	loud	$23 \pm 1^\circ\text{C}$	0	$\sim 0$
speaking <sup>a</sup>	loud	$50 \pm 5\%$ RH	1	$<0.01$
speaking <sup>a</sup>	loud	ACH of $9\text{ h}^{-1}$	4	$<0.01$
speaking <sup>a</sup>	loud		9	$<0.01$
coughing <sup>b</sup>	loud		1	$<0.01$
coughing <sup>b</sup>	loud		4	$<0.01$
coughing <sup>b</sup>	loud		9	$<0.01$
breathing <sup>c</sup>	–		9	$<0.01$

<sup>a</sup> The phrase “stay healthy” was repeatedly spoken in a loud voice (maximum 83 dB at the distance of 40 cm; average 77 dB) with 2–4 s of pause in between the phrases in 10-min “speaking” phase.

<sup>b</sup> The “coughing” was repeated with similar loudness (maximum 86 dB at the distance of 40 cm; average 72 dB) with 2–4 s of pause in 10-min “coughing” phase.

<sup>c</sup> The inhalation and exhalation with both mouth and nose.

<sup>d</sup> ACH: air change per hour ( $\text{h}^{-1}$ ).

<sup>e</sup> The air velocity near the laser sheet in “decay” phase is almost 0 m/s by a hot wire anemometer, but air currents are still present ( $<0.01\text{ m/s}$  estimated by the movements of aerosols) even in stagnant air.

hold the upper part of the speaker body in a relatively clean environment before opening and speaking into the inner small re-sealable zipper bag, which was attached to the speaking hole of the chamber. The relatively clean environment in the outer large bag allowed the speaker to clean his/her lung during the background phase. The outer large bag can also prevent direct contact between the opening of the inner small bag and the untreated air in the lab given that any slight body movement or indoor air turbulence would result in potential contamination of the chamber during the speaking phase. In the speaking phase, only the front part of the speaker’s face (i.e., the nose and mouth) was closely attached to the opening of the inner small bag. As such, possible contamination due to other human body parts (e.g., hair) was negligible, which was also verified by the obvious difference in aerosol results between the speaking and breathing cases (Fig. A6). Moreover, the high pressure within the chamber forces air to flow out of the speaking hole, through the inner small bag followed by the outer large bag, which was also important to avoid the potential contamination of the chamber. More details about the two-layered sealing bags and experimental procedure can be found in the Appendix.

Under the Covid-19 restrictions imposed by the University, lab access was restricted to only research staff who were authorized users. To avoid the possible transmission of Covid-19, only a subject, one of the authors of this work, was tested for the 8 cases (Table 1) with repeats of at least 3 times. The subject had no history of respiratory disease or symptoms. The phrase “stay healthy” was chosen for its effectiveness in generating a large number of droplets and aerosols [15].

## 3. Results

### 3.1. Decay and lifetime of aerosols from speaking or coughing

The lifetime of the aerosols was first recorded in stagnant air. Subsequently, three different ventilation conditions were considered where the air change per hour (ACH) was set as 1, 4, and  $9\text{ h}^{-1}$ , corresponding to typical home (natural ventilation), office (common mechanical ventilation), and crowded scenarios (strong mechanical ventilation), respectively [27]. It was found that the aerosols expelled from speaking decreased exponentially and remained suspended for up to 9 h in stagnant air after the end of speaking (Fig. 2), which are captured at 30, 120, 360, 565 min by LSO (Fig. 2B, C, 2E, and 2F). For non-stagnant

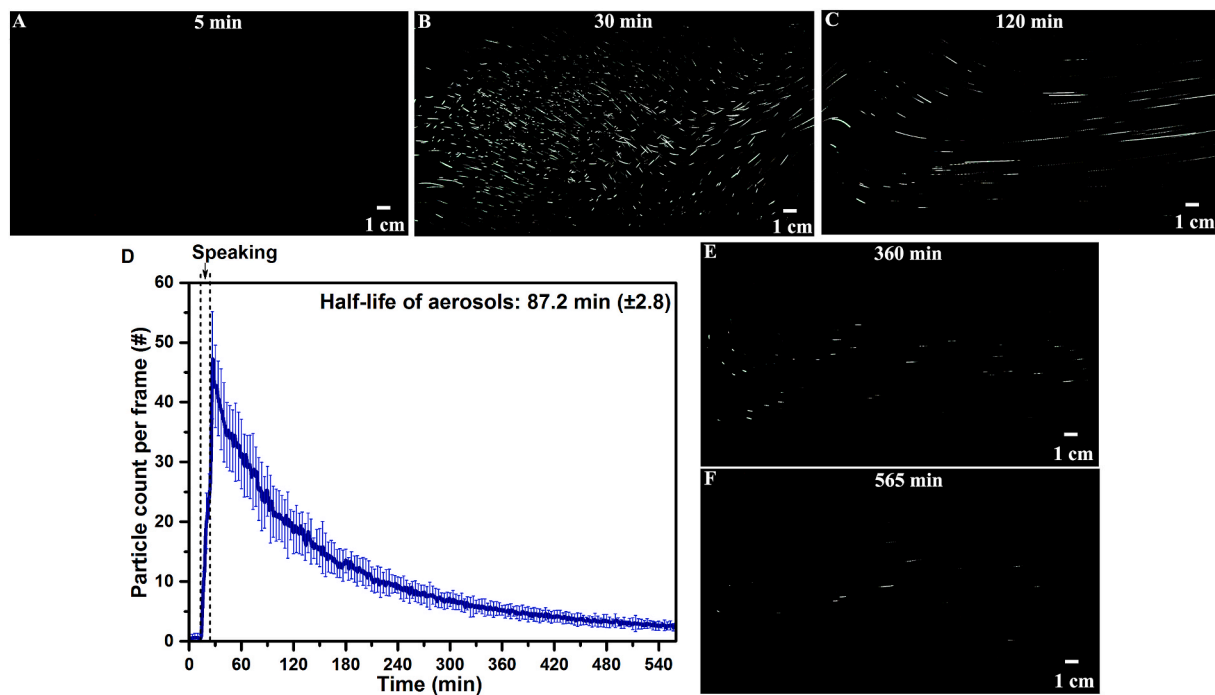


**Fig. 2.** Decay and lifetime of aerosols from speaking in stagnant air. (D) The decay of aerosols from speaking in terms of particle count per frame by light scattering observation (100-s moving average for the original data) across “background” (14 min), “speaking” (~10 min), and “decay” (for 9 h in stagnant air) phases with five repeats. In the speaking phase, the phrase “stay healthy” was repeatedly spoken in a loud voice (maximum 83 dB at the distance of 40 cm; average 77 dB) with 2–4 s of pause in between the phrases. Accumulated images of 500 successive frames (20 s) for one of the tests at (A) 5 min, (B) 30 min, (C) 120 min, (E) 360 min, and (F) 565 min. A movie is available online at <https://doi.org/10.5281/zenodo.4703075>.

environments, the number concentration of aerosols from speaking or coughing displayed an exponential decay over time across all experimental conditions (Fig. 3, Figs. A4–A5 of Appendix), and finally decreased to near background levels ( $0\text{--}1.2 \times 10^{-3} \text{ \#}/\text{cm}^3$ ) after about 4 h (ACH:  $1 \text{ h}^{-1}$ ), 1.2 h (ACH:  $4 \text{ h}^{-1}$ ), and 0.5 h (ACH:  $9 \text{ h}^{-1}$ ), measured by the optical particle sizer for particles from 0.3 to  $10 \text{ \mu m}$  (Fig. 3). For the half-life of aerosols, it is obvious that it declined with the increase in ACH from 87.2 min (ACH:  $0 \text{ h}^{-1}$ ), 28–40 min (ACH:  $1 \text{ h}^{-1}$ ), 10–14 min (ACH:  $4 \text{ h}^{-1}$ ), to 4–6 min (ACH:  $9 \text{ h}^{-1}$ ) (Figs. 2D and 3B). The half-life of aerosols from coughing was slightly higher than that of speaking by 3.6%–37.8 % in most cases, regardless of the measurement methods (Fig. 3B).

### 3.2. Time-resolved size distribution of aerosols from speaking or coughing

The size distribution of aerosols after dehydration from speaking was across the wide size range from 10 nm to  $8 \text{ \mu m}$  (Fig. 4) under ACH of  $4 \text{ h}^{-1}$ , and there was no noticeable difference between speaking and coughing (Fig. 4, Fig. A6 of Appendix). The distribution of aerosols appears random in all 13 size bins obtained from the scanning mobility particle sizer (10–420 nm), without a specific mode of particles (Fig. 4A, Fig. A6). In contrast, most aerosols measured by the optical particle sizer (0.3– $10 \text{ \mu m}$ ) were concentrated from 0.3 to  $0.7 \text{ \mu m}$  (Fig. 4B, Fig. A6). As expected, the aerosols with larger diameters from 2.5 to  $10 \text{ \mu m}$  disappeared earlier, and smaller aerosols (0.3– $2 \text{ \mu m}$ ) remained suspended in the air till the end of their lifetime (Fig. 4B, Fig. A6, Fig. 3A). Also, aerosols from normal breathing were investigated and there were few data points observed (Fig. A6) compared to speaking or coughing.

## 4. Discussion

Our results indicate that the long-time (hours) and long-distance airborne transmission of respiratory viruses (e.g., SARS-CoV-2) are plausible via air movement since the aerosols expelled from speaking

can remain suspended in the air for up to 9 h in a stagnant environment with a half-life of 87.2 min. Calculations predict that a  $1\text{-}\mu\text{m}$  particle will take about 7.4 h to settle to the ground from 0.8 m in a stagnant environment based on Stokes’ law [10]. Undeniably, the complete proof of the airborne transmission must include another two necessary evidences: high viral loads are existing in the oral fluids and upper respiratory tract of patients [28,29], and the SARS-CoV-2 virus can remain viable in aerosols for 3 h, which was reported recently using “artificial” aerosols generated by a 3-jet Collision nebulizer [30].

For the lifetime of speech aerosols, in a recent study, the lifetime was measured via LSO in a stagnant environment (a  $0.23 \text{ m}^3$  of cardboard box), with a half-life of 8–14 min reported [15]. However, the size information of aerosols was not quantitatively obtained by the LSO measurements. In contrast, a bigger stainless-steel chamber ( $0.5 \text{ m}^3$ ) was adopted with a longer time of speaking (10 min) in our study as compared to the 25 s of speaking in their study. In addition, via both LSO and aerosol sampling measurements, we are able to obtain both the lifetime and size distribution of speech aerosols under a stagnant environment and three different levels of ventilation. As compared to the study, the half-life values of aerosols are longer (4–87.2 min) in our study. One possible reason is that most aerosols evaporated into smaller diameters during the long 10-min speaking phase. Another possible reason is that there is less aerosol loss due to deposition from contact or static electricity in a bigger stainless-steel chamber.

With the size-resolved number concentration of aerosols at the end of the “speaking phase” (Fig. 4B, Fig. A6) and the volume of the chamber, it is estimated that 10-min loud speaking or independent coughing, produced 0.25 (413 per second) or 0.19 (315 per second) millions of aerosols in the size range of 0.3– $10 \text{ \mu m}$ , respectively (Fig. 4C, Figs. A7A and A7B). In another study, the emission rate was reported to be 330 particles per second in the size range of 0.3– $20 \text{ \mu m}$  for the “aah” vocalization [31]. For SARS-Cov-2, estimates using the average viral load in oral fluid ( $7 \times 10^6$  copies per milliliter) suggest that 10-min loud speaking or coughing could generate 64 (21586 for the maximum virus



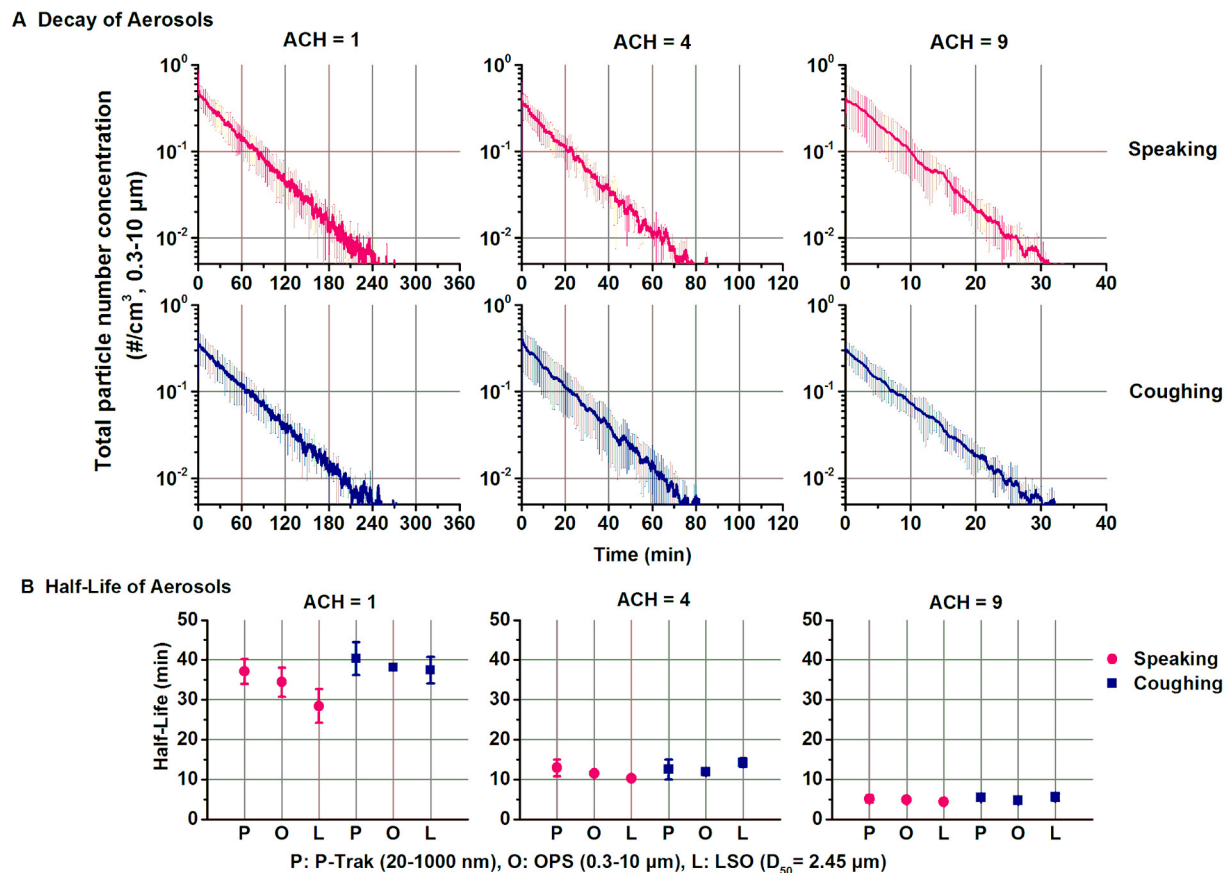


**Fig. 3.** Decay and half-life of aerosols from speaking and coughing under different ventilations. Panel (A) The decay of aerosols for both the speaking and coughing in terms of total particle number concentration (0.3–10 μm by optical particle sizer, OPS, 100-s moving average for the original data) in the “decay” phase under three different ventilation conditions (air change per hour, ACH: 1, 4, and 9 h<sup>-1</sup>) with three repeats. (B) The half-life of the aerosols based on the exponential decay rates of particle concentrations in the chamber. “O” indicates that the half-life is obtained by OPS, “P” measured by ultrafine particle counter (P-Trak, 20–1000 nm), and “L” by the light scattering observation (LSO, D<sub>50</sub> = 2.45 μm, D<sub>50</sub> means that 50 % of particles are visible, which is also regarded as minimum visible particle size, see Figs. A2–A3 of Appendix A). Plots show the means and standard errors across three replicates. Note that decay of aerosols demonstrated in panel A is by OPS measurement since its sensitivity is better than that of LSO, and corresponding results measured by the LSO and P-Trak are shown in Figs. A4–A5 of the Appendix.

load of  $2.35 \times 10^9$  copies per milliliter) or 27 (8988) virus-laden aerosols in the size range of 0.3–2 μm that remain suspended almost until the end of the lifetime of the aerosols, respectively (Fig. 4B and D) [15]. A mathematical model predicted that only a single cough may generate as many as 1855 virus-containing particles that can remain airborne after 10 s (for viral load in oral fluid:  $2.35 \times 10^9$  copies per milliliter) [32] based on the droplet size distribution measured by Chao et al. [26]. In this work, a single cough was estimated to produce about 239 virus-containing particles (28707 by 10-min coughing or ~120 coughs) in the size range of 0.3–10 μm using the same viral load.

The aerosols in size bin of 0.3–2 μm, in which aerosols have a higher possibility to carry more viruses than smaller aerosols (<0.3 μm) (Fig. A7C) and their lifetime being relatively longer than larger aerosols (>2 μm) (Fig. 4B), are likely to be the crucial medium to spread infectious respiratory diseases (Fig. 4D), especially in the super-speeding events of SARS-CoV-2 [5]. The infection risk of SARS-CoV-2 via the small aerosols (0.3–2 μm) compared to larger aerosols (e.g., 2–10 μm after dehydration) or droplet deposition route (e.g., >20 μm after dehydration) needs to be further evaluated using risk assessment models (e.g., AirCoV2) for various indoor scenarios (e.g., a cafe) [17,23,33,34]. Also, using virus-laden aerosols generated by infected humans or other animals is recommended to evaluate the transmissibility of reparatory diseases [35,36]. More subjects need to be tested in the future using the methodology proposed in this work considering the variance between different persons [37].

To obtain the minimum visible droplets in LSO, calibrations using

standard monodisperse droplets were conducted in this work, and D<sub>50</sub> was about 2.45 μm in our study (Figs. A2–A3). For the aerosol diameter in LSO, even though the counting efficiency is lower than 50 % for aerosols less than 2.45 μm, aerosols captured in Fig. 2 were expected to be in the size range of 0.6–2.5 μm (Fig. 2). It is worth noting that the aerosol concentration in the 252-cm<sup>3</sup> observation window of LSO is considerably lower than OPS measurements by about 9 times. This is because the counting efficiency of the LSO is lower than 50 % for aerosols less than 2.45 μm and most speech aerosols varied from 0.3 to 2 μm. For instance, the counting efficiency of LSO was estimated to be only 16.7 % for 1-μm droplets compared to the OPS (Fig. A3k). In essence, even though LSO and OPS use the same technique of light scattering, the sensitivity of OPS was higher than that of LSO. However, the LSO technique provided real-time visual evidence of aerosols in the air [15], which did not affect the stagnant air condition due to sampling and had no particle loss unlike the sampling process of OPS.

Although our results are not from patients infected by respiratory viruses, the accurate experimental evidence reported here fills an important gap for the possibility of the long-distance and long-time airborne transmission of SARS-CoV-2. This work indicates that 2 m of social distance is not enough to prevent airborne transmission route, and new control measures targeting the generation (e.g., wear masks) [21, 38], accumulation (e.g., ventilation or filtration) [39,40], and inhalation of aerosols (e.g., wear masks) [41] should be considered in the battle against COVID-19 and future new infectious respiratory diseases.

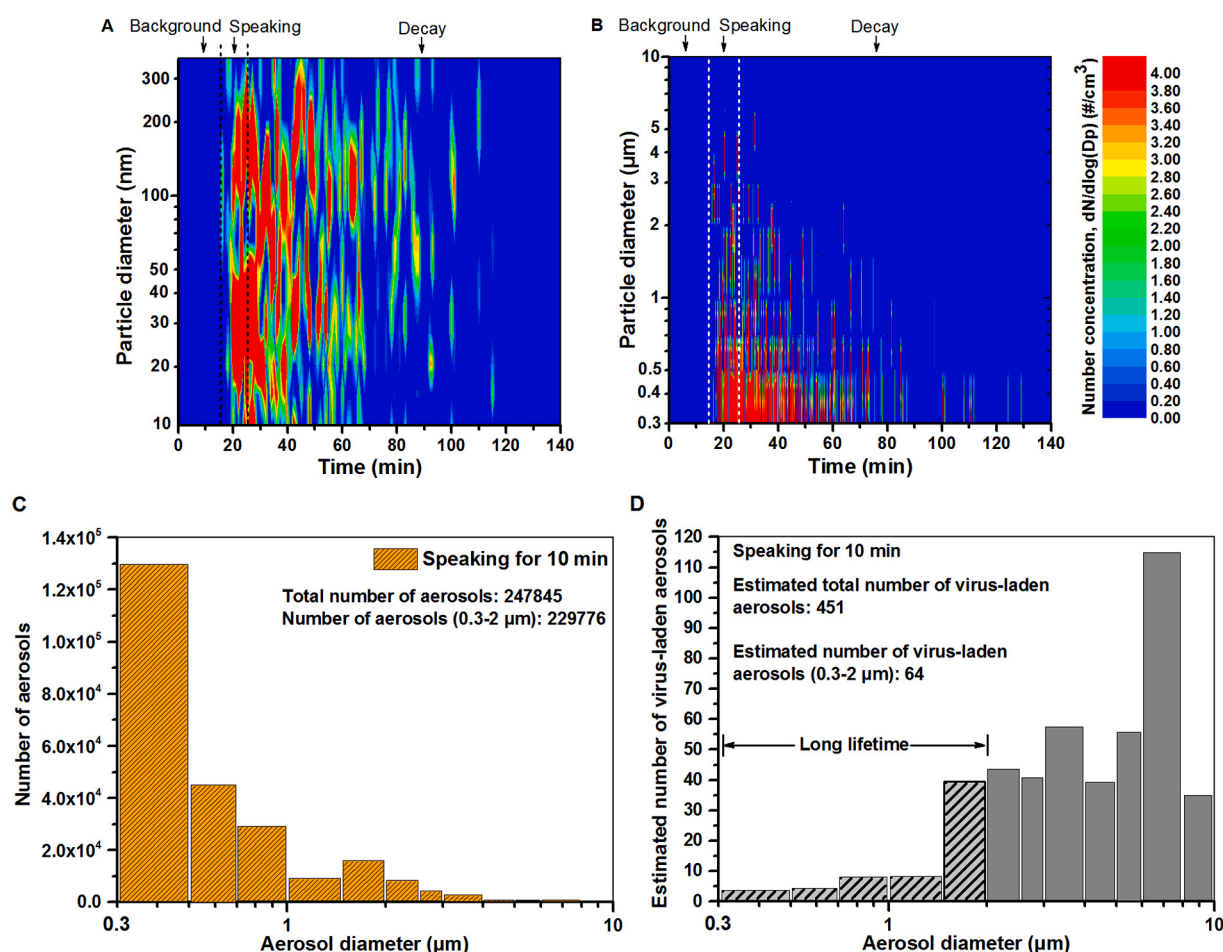


**Fig. 4.** Time-resolved size distribution of aerosols from speaking. Time-resolved size distribution of aerosols across “background” (14 min), “speaking” (~10 min), and “decay” measured by (A) scanning mobility particle sizer for particles from 10 to 420 nm, and (B) optical particle sizer (OPS) for particles from 0.3 to 10  $\mu\text{m}$  in the chamber (air change per hour:  $4\text{ h}^{-1}$ ). Size distributions under different ventilations are shown in Fig. A6 of Appendix. (C) Average size-resolved number of aerosols in 12 size bins of optical particle sizer from the 10-min speaking (average across the 9 tests). (D) Estimated size-resolved number of SARS-CoV-2 virus-laden aerosols from 10-min speaking based on average particle size distribution by OPS (Fig. A7A of Appendix) and average virus load of oral fluid of COVID-19 patients ( $7 \times 10^6$  copies per milliliter), assuming the size of aerosols measured shrinks to 20 % of its original size due to dehydration [15].

## 5. Conclusions

The present study obtained the accurate lifetime and size of aerosol from speaking and coughing in stagnant air and under three different levels of ventilation. Speech aerosols from speaking can linger in stagnant air for up to 9 h with a half-life of 87.2 min. The half-life of the aerosols declined with the increase in air change per hour from 28 to 40 min ( $1\text{ h}^{-1}$ ), 10–14 min ( $4\text{ h}^{-1}$ ), to 4–6 min ( $9\text{ h}^{-1}$ ). The aerosols in the size range of about 0.3–2  $\mu\text{m}$  had the longest lifetime compared to larger aerosols (2–10  $\mu\text{m}$ ). These results suggest that speech aerosols have the potential to transmit respiratory viruses across long duration (hours), and long-distance (over social distance) through the airborne route. This information is important for researchers and engineers to simulate the airborne dispersion of viruses and to design new ventilation systems.

## Declaration of competing interest

The authors declare that they have no known competing financial interests or personal relationships that could have appeared to influence the work reported in this paper.

## Acknowledgments

This study was funded by the start-up grant under Nanyang

Technological University (04INS000329C160). Shirun Ding would like to acknowledge Nanyang Technological University for funding his Ph.D and thank the Singapore Centre for 3D Printing on experimental support.

## Appendix A. Supplementary data

Supplementary data to this article can be found online at <https://doi.org/10.1016/j.buildenv.2021.108239>.

## Data availability statement

The data are available from the corresponding author upon reasonable request.

## CRediT authorship contribution statement

S. Ding: Conceptualization, investigation, writing-original draft; Z. W. Teo: Investigation, writing-review; M.P. Wan: Conceptualization, supervision; B.F. Ng: Conceptualization, funding, writing-review & editing, supervision.

## References

- [1] R. Tellier, Y. Li, B.J. Cowling, J.W. Tang, Recognition of aerosol transmission of infectious agents: a commentary, *BMC Infect. Dis.* 19 (2019) 1–9.
- [2] L. Morawska, J.W. Tang, W. Bahnfleth, P.M. Bluyssen, A. Boerstra, G. Buonanno, J. Cao, S. Dancer, A. Floto, F. Franchimon, How can airborne transmission of COVID-19 indoors be minimised? *Environ. Int.* 142 (2020), 105832.
- [3] L. Morawska, J. Allen, W. Bahnfleth, P.M. Bluyssen, A. Boerstra, G. Buonanno, J. Cao, S.J. Dancer, A. Floto, F. Franchimon, A paradigm shift to combat indoor respiratory infection, *Science* 372 (2021) 689–691, 80–.
- [4] P.G. da Silva, M.S.J. Nascimento, R.R.G. Soares, S.I. V Sousa, J.R. Mesquita, Airborne spread of infectious SARS-CoV-2: moving forward using lessons from SARS-CoV and MERS-CoV, *Sci. Total Environ.* (2020) 142802.
- [5] S.L. Miller, W.W. Nazaroff, J.L. Jimenez, A. Boerstra, G. Buonanno, S.J. Dancer, J. Kurnitski, L.C. Marr, L. Morawska, C. Noakes, Transmission of SARS-CoV-2 by inhalation of respiratory aerosol in the Skagit Valley Chorale superspreading event, *Indoor Air* (2020).
- [6] Y. Li, H. Qian, J. Hang, X. Chen, P. Cheng, H. Ling, S. Wang, P. Liang, J. Li, S. Xiao, Probable airborne transmission of SARS-CoV-2 in a poorly ventilated restaurant, *Build. Environ.* 196 (2021) 107788.
- [7] J.F.-W. Chan, C.C.-Y. Yip, K.K.-W. To, T.H.-C. Tang, S.C.-Y. Wong, K.-H. Leung, A. Y.-F. Fung, A.C.-K. Ng, Z. Zou, H.-W. Tsoi, Improved molecular diagnosis of COVID-19 by the novel, highly sensitive and specific COVID-19-RdRp/Hel real-time reverse transcription-PCR assay validated in vitro and with clinical specimens, *J. Clin. Microbiol.* 58 (2020).
- [8] A.L. Rasmussen, S. V Popescu, SARS-CoV-2 transmission without symptoms, *Science* 371 (2021) 1206–1207, 80–.
- [9] Y. Liu, Z. Ning, Y. Chen, M. Guo, Y. Liu, N.K. Gali, L. Sun, Y. Duan, J. Cai, D. Westerdahl, Aerodynamic analysis of SARS-CoV-2 in two Wuhan hospitals, *Nature* 582 (2020) 557–560.
- [10] G.A. Somsen, C. van Rijn, S. Kooij, R.A. Bem, D. Bonn, Small droplet aerosols in poorly ventilated spaces and SARS-CoV-2 transmission, *Lancet Respir. Med.* 8 (2020) 658–659.
- [11] D. Lewis, Is the coronavirus airborne? Experts can't agree, *Nature* 580 (2020) 175.
- [12] L. Morawska, J. Cao, Airborne transmission of SARS-CoV-2: the world should face the reality, *Environ. Int.* 139 (2020) 105730.
- [13] C.X. Gao, Y. Li, J. Wei, S. Cotton, M. Hamilton, L. Wang, B.J. Cowling, Multi-route respiratory infection: when a transmission route may dominate, *Sci. Total Environ.* 752 (2021) 141856.
- [14] Y. Li, Basic routes of transmission of respiratory pathogens—a new proposal for transmission categorization based on respiratory spray, inhalation, and touch, *Indoor Air* 31 (2021) 3.
- [15] V. Stadnytskyi, C.E. Bax, A. Bax, P. Anfinrud, The airborne lifetime of small speech droplets and their potential importance in SARS-CoV-2 transmission, *Proc. Natl. Acad. Sci. Unit. States Am.* 117 (2020) 11875–11877.
- [16] M. Richard, A. Kok, D. de Meulder, T.M. Bestebroer, M.M. Lamers, N.M.A. Okba, M.F. van Vliening, B. Rockx, B.L. Haagmans, M.P.G. Koopmans, SARS-CoV-2 is transmitted via contact and via the air between ferrets, *Nat. Commun.* 11 (2020) 1–6.
- [17] W. Chen, N. Zhang, J. Wei, H.-L. Yen, Y. Li, Short-range airborne route dominates exposure of respiratory infection during close contact, *Build. Environ.* 176 (2020) 106859.
- [18] W.H. Organization, Modes of Transmission of Virus Causing COVID-19: Implications for IPC Precaution Recommendations: Scientific Brief, 27 March 2020, World Health Organization, 2020.
- [19] Q. Li, X. Guan, P. Wu, X. Wang, L. Zhou, Y. Tong, R. Ren, K.S.M. Leung, E.H.Y. Lau, J.Y. Wong, Early transmission dynamics in Wuhan, China, of novel coronavirus-infected pneumonia, *N. Engl. J. Med.* (2020).
- [20] S. Tang, Y. Mao, R.M. Jones, Q. Tan, J.S. Ji, N. Li, J. Shen, Y. Lv, L. Pan, P. Ding, Aerosol transmission of SARS-CoV-2? Evidence, prevention and control, *Environ. Int.* 144 (2020) 106039.
- [21] K.A. Prather, C.C. Wang, R.T. Schooley, Reducing transmission of SARS-CoV-2, *Science* 84 368 (2020) 1422–1424.
- [22] M. Yao, L. Zhang, J. Ma, L. Zhou, On airborne transmission and control of SARS-CoV-2, *Sci. Total Environ.* 731 (2020) 139178.
- [23] G. Buonanno, L. Stabile, L. Morawska, Estimation of airborne viral emission: quanta emission rate of SARS-CoV-2 for infection risk assessment, *Environ. Int.* 141 (2020) 105794.
- [24] B. Wang, H. Wu, X.-F. Wan, Transport and fate of human expiratory droplets—a modeling approach, *Phys. Fluids* 32 (2020) 83307.
- [25] K.P. Fennelly, Particle sizes of infectious aerosols: implications for infection control, *Lancet Respir. Med.* (2020).
- [26] C.Y.H. Chao, M.P. Wan, L. Morawska, G.R. Johnson, Z.D. Ristovski, M. Hargreaves, K. Niemeyer, S. Corbett, Y. Li, X. Xie, Characterization of expiration air jets and droplet size distributions immediately at the mouth opening, *J. Aerosol Sci.* 40 (2009) 122–133.
- [27] R. and A.-C.E. (ASHRAE. American Society of Heating, The standards for ventilation and indoor air quality. ANSI/ASHRAE Standard 62.1-2019. Ventilation for Acceptable Indoor Air Quality, 2019.
- [28] Y. Bai, L. Yao, T. Wei, F. Tian, D.-Y. Jin, L. Chen, M. Wang, Presumed asymptomatic carrier transmission of COVID-19, *Jama* 323 (2020) 1406–1407.
- [29] R. Wölfel, V.M. Corman, W. Guggemos, M. Seilmaier, S. Zange, M.A. Müller, K. Niemeyer, T.C. Jones, P. Vollmar, C. Rothe, Virological assessment of hospitalized patients with COVID-2019, *Nature* 581 (2020) 465–469.
- [30] N. Van Doremalen, T. Bushmaker, D.H. Morris, M.G. Holbrook, A. Gamble, B. N. Williamson, A. Tamin, J.L. Harcourt, N.J. Thornburg, S.I. Gerber, Aerosol and surface stability of SARS-CoV-2 as compared with SARS-CoV-1, *N. Engl. J. Med.* 382 (2020) 1564–1567.
- [31] L. Morawska, G.R. Johnson, Z.D. Ristovski, M. Hargreaves, K. Niemeyer, S. Corbett, C.Y.H. Chao, Y. Li, D. Katoshevski, Size distribution and sites of origin of droplets expelled from the human respiratory tract during expiratory activities, *J. Aerosol Sci.* 40 (2009) 256–269.
- [32] Y. Wang, G. Xu, Y.-W. Huang, Modeling the load of SARS-CoV-2 virus in human expelled particles during coughing and speaking, *PLoS One* 15 (2020), e0241539.
- [33] M.P. Wan, C.Y.H. Chao, Transport Characteristics of Expiratory Droplets and Droplet Nuclei in Indoor Environments with Different Ventilation Airflow Patterns, 2007.
- [34] J. Schijven, L.C. Vermeulen, A. Swart, A. Meijer, E. Duizer, A.M. de Roda Husman, Quantitative microbial risk assessment for airborne transmission of SARS-CoV-2 via breathing, speaking, singing, coughing, and sneezing, *Environ. Health Perspect.* 129 (2021) 47002.
- [35] D.K. Milton, M.P. Fabian, B.J. Cowling, M.L. Grantham, J.J. McDevitt, Influenza virus aerosols in human exhaled breath: particle size, culturability, and effect of surgical masks, *PLoS Pathog.* 9 (2013), e1003205.
- [36] S.F. Sia, L.-M. Yan, A.W.H. Chin, K. Fung, K.-T. Choy, A.Y.L. Wong, P. Kaewpreedee, R.A.P.M. Perera, L.L.M. Poon, J.M. Nicholls, Pathogenesis and transmission of SARS-CoV-2 in golden hamsters, *Nature* 583 (2020) 834–838.
- [37] L. Morawska, C. He, G. Johnson, R. Jayaratne, T. Salthammer, H. Wang, E. Uhde, T. Bostrom, R. Modini, G. Ayoko, An investigation into the characteristics and formation mechanisms of particles originating from the operation of laser printers, *Environ. Sci. Technol.* 43 (2009) 1015–1022.
- [38] P. Anfinrud, V. Stadnytskyi, C.E. Bax, A. Bax, Visualizing speech-generated oral fluid droplets with laser light scattering, *N. Engl. J. Med.* 382 (2020) 2061–2063.
- [39] Q. Chen, Can we migrate COVID-19 spreading risk? *Front. Environ. Sci. Eng.* 15 (2021) 1–4.
- [40] E. Kujundzic, F. Matalkah, C.J. Howard, M. Hernandez, S.L. Miller, UV air cleaners and upper-room air ultraviolet germicidal irradiation for controlling airborne bacteria and fungal spores, *J. Occup. Environ. Hyg.* 3 (2006) 536–546.
- [41] A. Davies, K.-A. Thompson, K. Giri, G. Kafatos, J. Walker, A. Bennett, Testing the efficacy of homemade masks: would they protect in an influenza pandemic? *Disaster Med. Public Health Prep.* 7 (2013) 413–418.